BCV
progetti s.r.l.

COLUMBUS PROJECT

MIRROR BLANK 8.4 mt diam F/1.14

FINITE ELEMENT MODEL IMPROVEMENT

Report N. 132 Rev.0
Milano, 1991, September

BCV progetti s.r.l.

INDEX

1.	INTRODUCTION: WHY A NEW F.E. MODEL?	pag. 3
2.	NEW NUMERICAL MODEL	pag. 6
3.	ENCLOSURES	pag. 7

1. INTRODUCTION: WHY A NEW F.E. MODEL?

The numerical model used just now for the primary mirrors of the Columbus telescope has been designed and tested in 1988 (see rep. N° 104). Then the model has been modified several times in order to adapt it to geometry changes, but the model design didn't change.
The mean features of such a model were:

- One quarter of the mirror, has been modelled.
- Shell elements (6 d.o.f each node).
- Four node layers in the mirror thickness.
- One node at the center of each cell only on the optical surface.

In this way we arrived to a numerical problem having a linear system of about 22000 unknowns and coefficient matrix greater than 130 Mb.

During these last years computer performances improve considerably and recently BCV progetti changes its system. As consequence it became possible, if necessary, to increase the dimension of our numerical models.
Since the extreme degree of precision required in this application it is interesting to check if it is usefull to refine the numerical model of the primary mirror.
The simplest way in order to refine the model is to increase the node number. If we try to use more than one element along each cell side the d.o.f. number increases too much, so the only way in order to refine the model is to increase the node number in the mirror thickness.

Being the axial supports number very big, the main component of the optical surface displacements is due to the rib shear strains and moreover to the bumps produced by the diffusion of the supporting forces in the ribs.
So it could be usefull to increase the number of the node layers in the rib thickness. In order to check that we appoint some numerical tests.

Two plane borosilicate sheets 12 mm thick, 880 mm long and having heigth respectively equal 400 and 800 mm have been modeled as reported in figures 1-2. Loads and constraints are those reported in figure 1:

- there is a support each 880 mm (on the mirror we have a support each 4 cell sides), at the extreme sides we have symmetry constraints in order to simulate an infinite sheet supported each 880 mm;

- The constraints have a finite dimension equal 66 mm (three node supported for each support). This in order to take into account the finite dimension of spreader load prints (70 mm diameter).
- Two loadings have been considered, the first one is represented in figure 1: the rib is loaded by concentrated loads, one reference load (100 N) each 110 mm; in the second loading the dead weigth of the rib acts (so it is a distributed load).

Since the discretization is quite refined, surely much more refined than that of the global model, we will use the results of the models in figures 1-2 as "exact" results.
Then we appointed the meshes in figures from 3 to 8, they are relative to the same ribs but:

- only one element in each rib width (110 mm) is used as in the global model
- four, five or six node layers have been used in the mirror thickness

The same loadings have been applied to all the models and obviously the same code (SAP V) and the same finite element (SHELL) of the global model have been used.
In the different models the following parameters have been compared:

- Upper nodes average displacements, named $\bar{V}$ in fig. 9; it is a parameter related to the average displacement of the whole zone above a support.
- Peak to valley of the displacements of the upper nodes, named ΔV in figure 9; it is a parameter representative of the ripples on the optical surface.

Obviously, since the loads applied are reference loads and not the real ones, it is not important the absolute value of such displacements but it is important the percentage difference between each parameter computed using simplified models (figures 3-8) and the corresponding on the refined models (fig. 1-2).
These percentage differences are reported between brackets in the following tables.

RIBS HEIGHT = 400 mm
LOADING N° 1 - CONCENTRATED LOADS

displac. component	refined model	4 node layers [nm]	5 node layers [nm]	6 node layers [nm]
$\bar{V}$	1183.	1019. (-13.9%)	1055. (-10.8%)	1073 (-9.3%)
ΔV	28.	12. (-57%)	20. (-29%)	23 (-18%)

RIBS HEIGHT = 800 mm LOADING N° 1 - CONCENTRATED LOADS				
displac. component	**refined model**	**4 node layers [nm]**	**5 node layers [nm]**	**6 node layers [nm]**
$\bar{V}$	1568.	1391. (-11.3%)	1453. (-7.3%)	1496 (-4.6%)
ΔV	0.	2.	0.	0.

RIBS HEIGHT = 400 mm LOADING N° 2 - DISTRIBUTED LOADS				
displac. component	**refined model**	**4 node layers [nm]**	**5 node layers [nm]**	**6 node layers [nm]**
$\bar{V}$	92.88	88.12 (-5.1%)	92.26 (-0.7%)	94.31 (+1.5%)
ΔV	3.26	1.41 (-57%)	2.23 (-32%)	2.7 (-17%)

RIBS HEIGHT = 800 mm LOADING N° 2 - DISTRIBUTED LOADS				
displac. component	**refined model**	**4 node layers [nm]**	**5 node layers [nm]**	**6 node layers [nm]**
$\bar{V}$	225.6	203.6 (-9.8%)	217.8 (-3.5%)	227.7 (+0.9%)
ΔV	0.0	0.4	0.0	0.0

The results reported above show that if the mirror thickness is 800 mm the model with only 4 node layers is quite refined for our purposes, but in the internal mirror zone, where the mirror thickness is approximately 400 mm. both $\bar{V}$ and ΔV are underestimated.
The model with 6 node layers permit to reduce from 57% to 17% the percentage difference on the ripples as regards the refined model.

So, in order to better estimate the displacements in the internal zone of the mirror, we decided to appoint a new model similar to the old one but with 6 node layers (five elements) on the mirror thickness. The node, at the center of each cell, on the optical surface has been restored progetti s.r.l.

(we suppressed it in the model described in rep. N° 125).
In this way we obtained a model of a quarter of the mirror having: 34632 degrees of fredom. The matrix coefficient of the linear system related to our problem is about 330 Mb big with a bandwidth equal to 1164.

2. NEW NUMERICAL MODEL

For the geometrical and mechanical characteristics we refer to those ones of previous numerical model, which are described in the Report n. 125 - October 1990.

The usual numerical checks have been performed in order to test the model, considering the mirror zenith pointing, constrained in axial direction as in figure 10 for the symmetrical load condition reported in figures 11.
We compared the axial displacements of three node terns on the upper plate and precisely the nodes:
1462, 2960, 4154
2673, 5668, 8056
4783, 7478, 11956
6284, 7183, 12866
which must have equal displacements because of the symmetry conditions.
The test results are reported in the following table. The displacements are measured in nanometers:

AXIAL DISPLACEMENTS (nm)										
NODE NUMBER	DISPL. LOAD. 1	DIFF.	DISPL. LOAD. 2	DIFF.	DISPL. LOAD. 3	DIFF.	DISPL. LOAD. 4	DIFF.	DISPL. LOAD. 5	DIFF.
1462	15269.	-	5384.	-	-120.	-	-1405.	-	-39237.	-
2960	15269.	0.	5384.	0.	-120.	0.	-1405.	0.	-39237	0.
4154	15270.	1.	5384.	0.	-120.	0.	-1405.	0.	-39239	2.
2673	5265.	-	3901.	-	2396.	-	474.	-	-37505.	-
5668	5265.	0.	3901.	0.	2396.	0.	474.	0.	-37506.	1.
8056	5267	2.	3902.	1.	2396.	0.	474.	0.	-37511.	5.
4783	-1833.	-	1922.	-	5746.	-	3077.	-	-49007.	-

BCV
progetti s.r.l.

AXIAL DISPLACEMENTS (nm)										
NODE NUMBER	DISPL. LOAD. 1	DIFF.	DISPL. LOAD. 2	DIFF.	DISPL. LOAD. 3	DIFF.	DISPL. LOAD. 4	DIFF.	DISPL. LOAD. 5	DIFF.
7478	-1834.	1.	1922.	0.	5747.	1.	3077.	0.	-49009.	2.
11956	-1830	3.	1923.	1.	5746.	0.	3077.	0.	-49007.	0.
6284	-3849.	-	1433.	-	6705.	-	4096.	-	-53285.	-
7183	-3850.	1.	1433.	0.	6705.	0.	4096.	0.	-53285.	0.
12866	-3845.	4.	1434.	1.	6703.	2.	4095.	1.	-53284.	1.

The check results seems us satisfactory.

3. ENCLOSURES

We enclose the drawings of finite element mesh.
The drawing 1 represents the back plate with the numbering of nodes and elements.
The drawing 2 represents a generic rib layer with the typical element numbering.
The drawing 3 represents a generic rib layer.
The drawing 4 represents the upper plate with the numbering of nodes and elements.

FIGURE 1

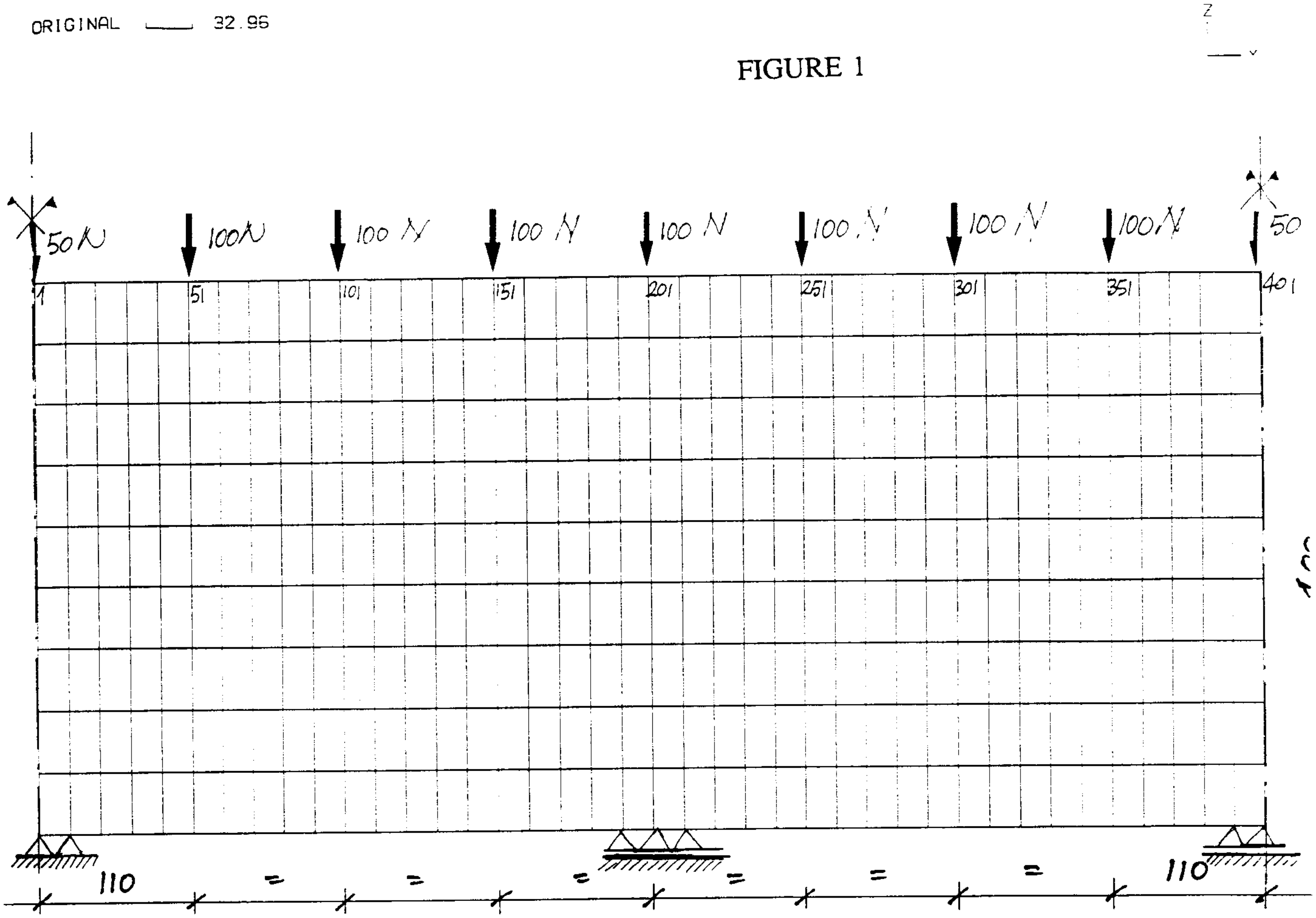

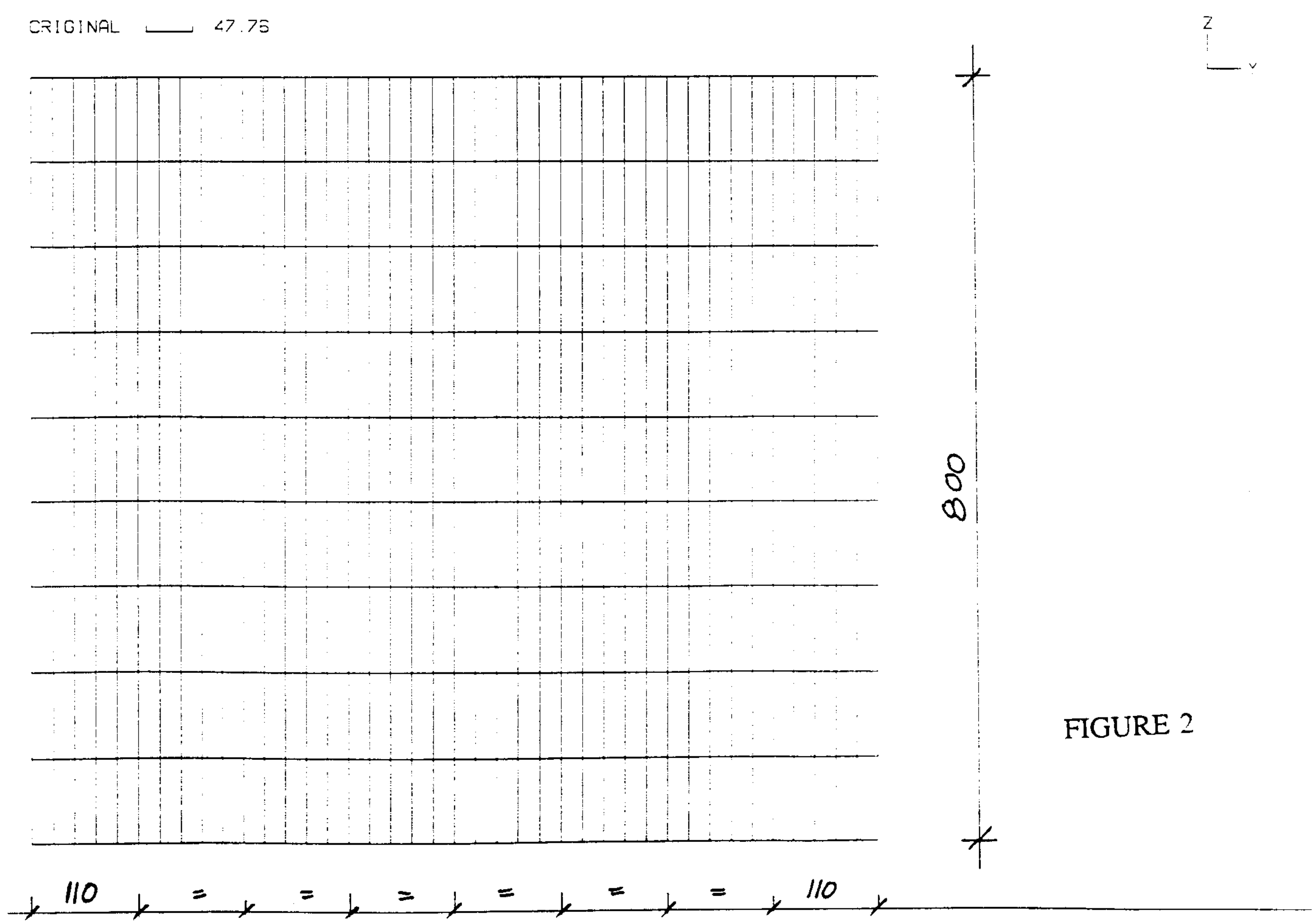

FIGURE 2

ORIGINAL 32.96

FIGURE 3
four node layers

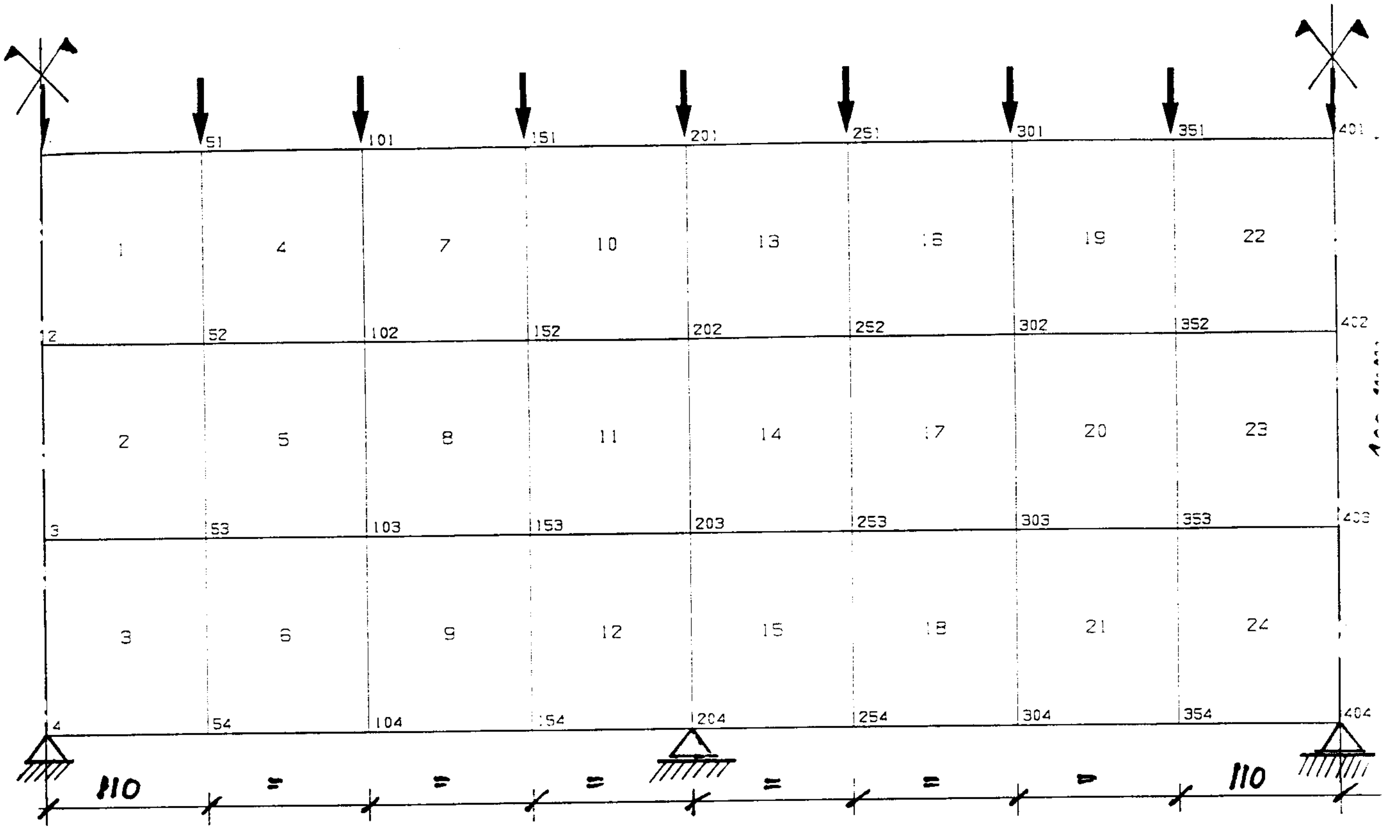

ORIGINAL 32.96

FIGURE 4
five node layers

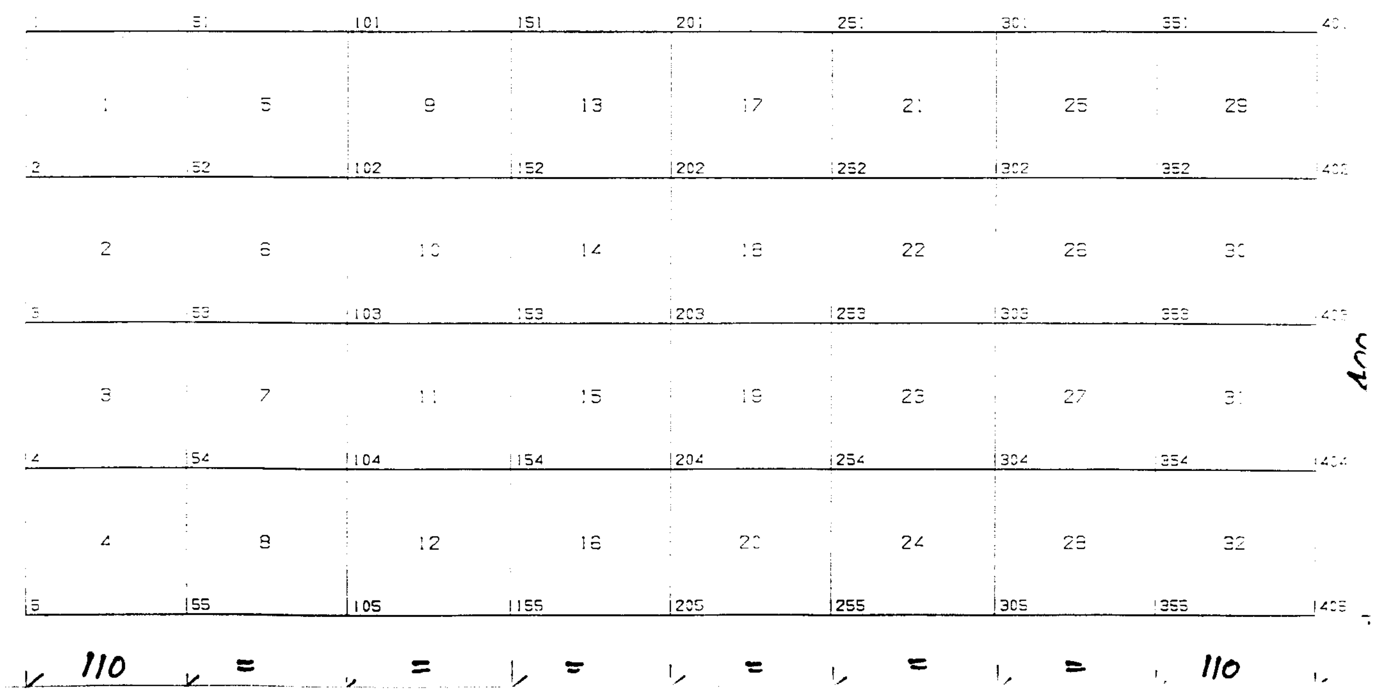

FIGURE 5
six node layers

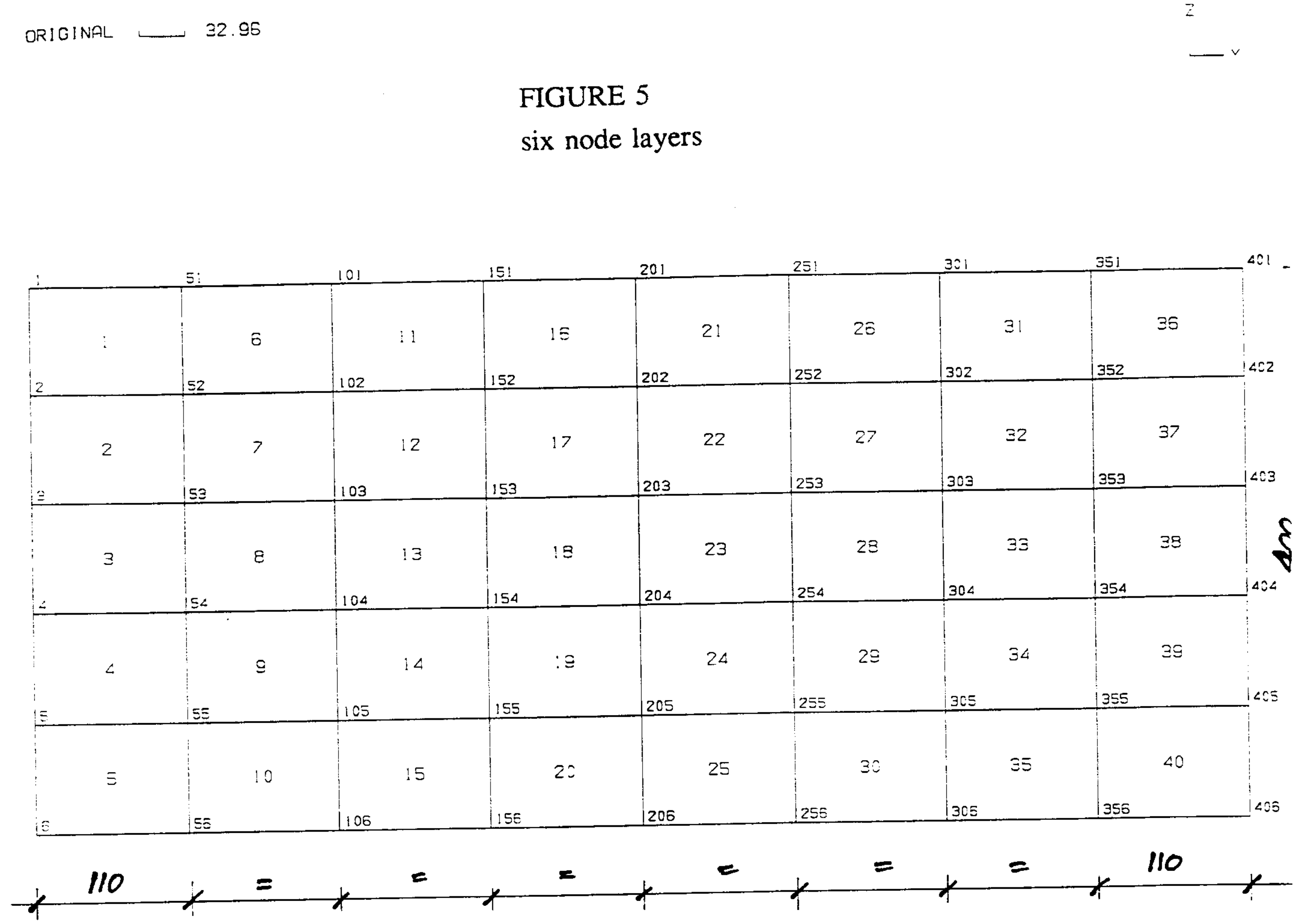

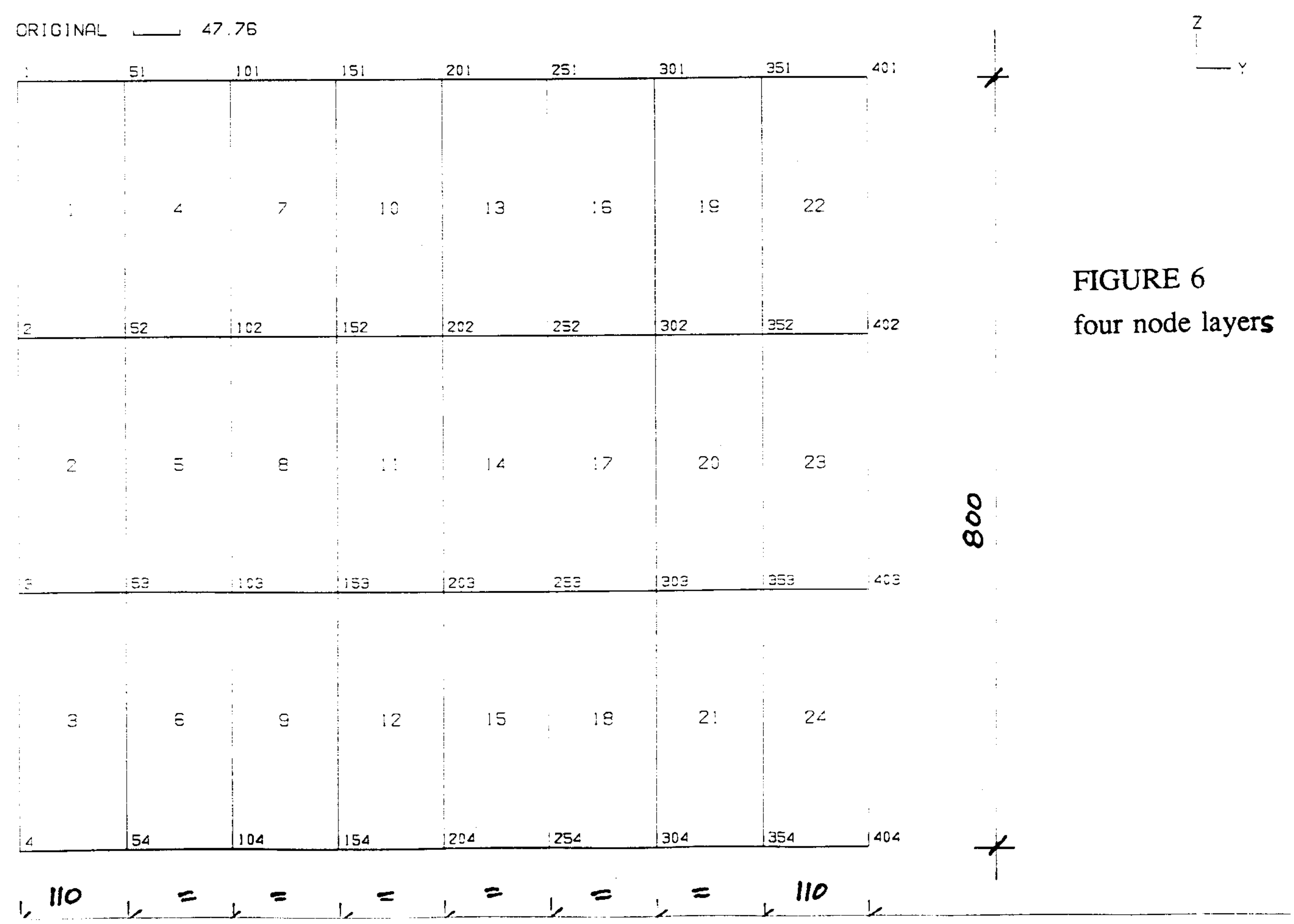

FIGURE 6
four node layers

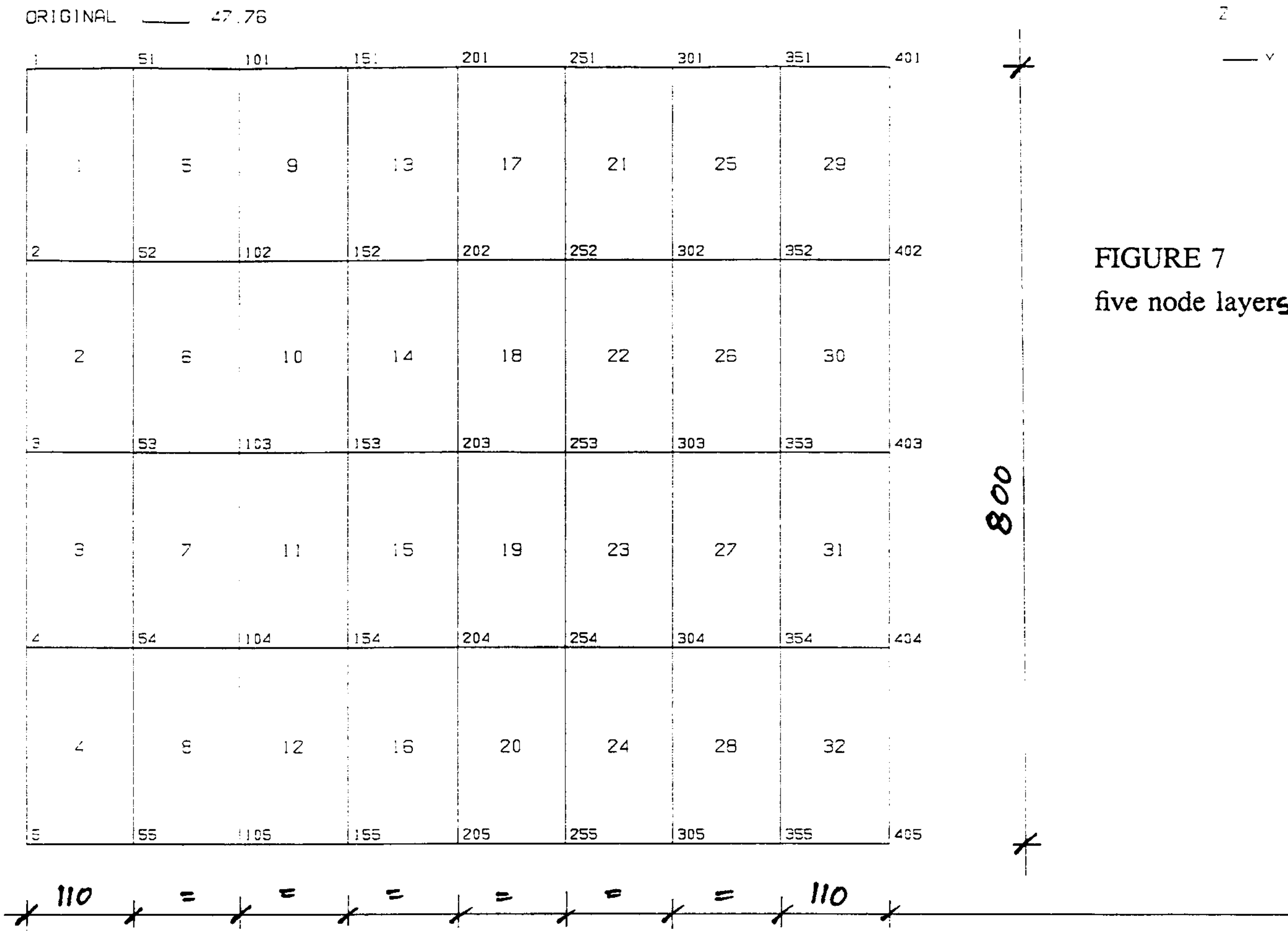

FIGURE 7
five node layers

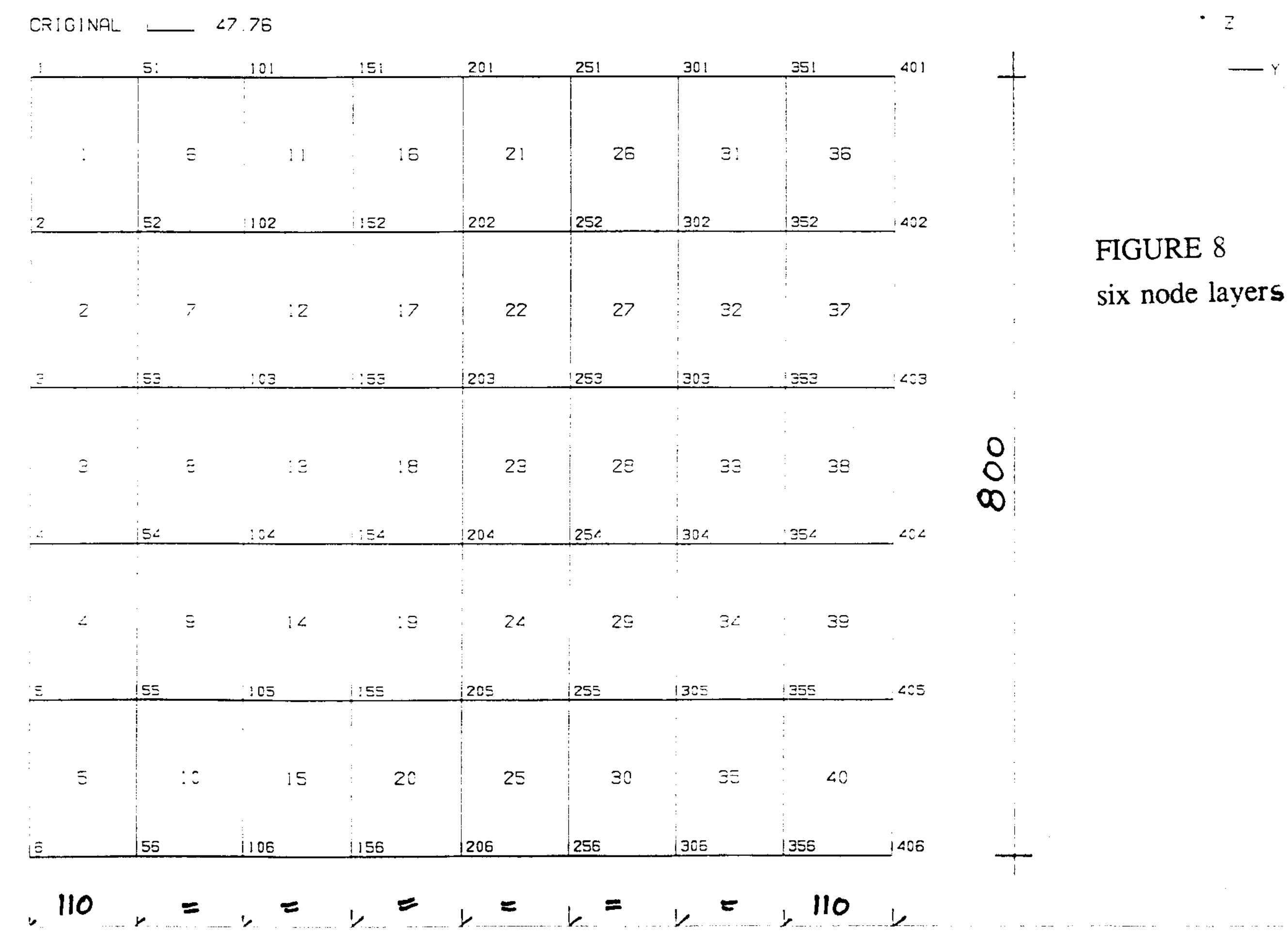

FIGURE 8
six node layers

FIGURE 9

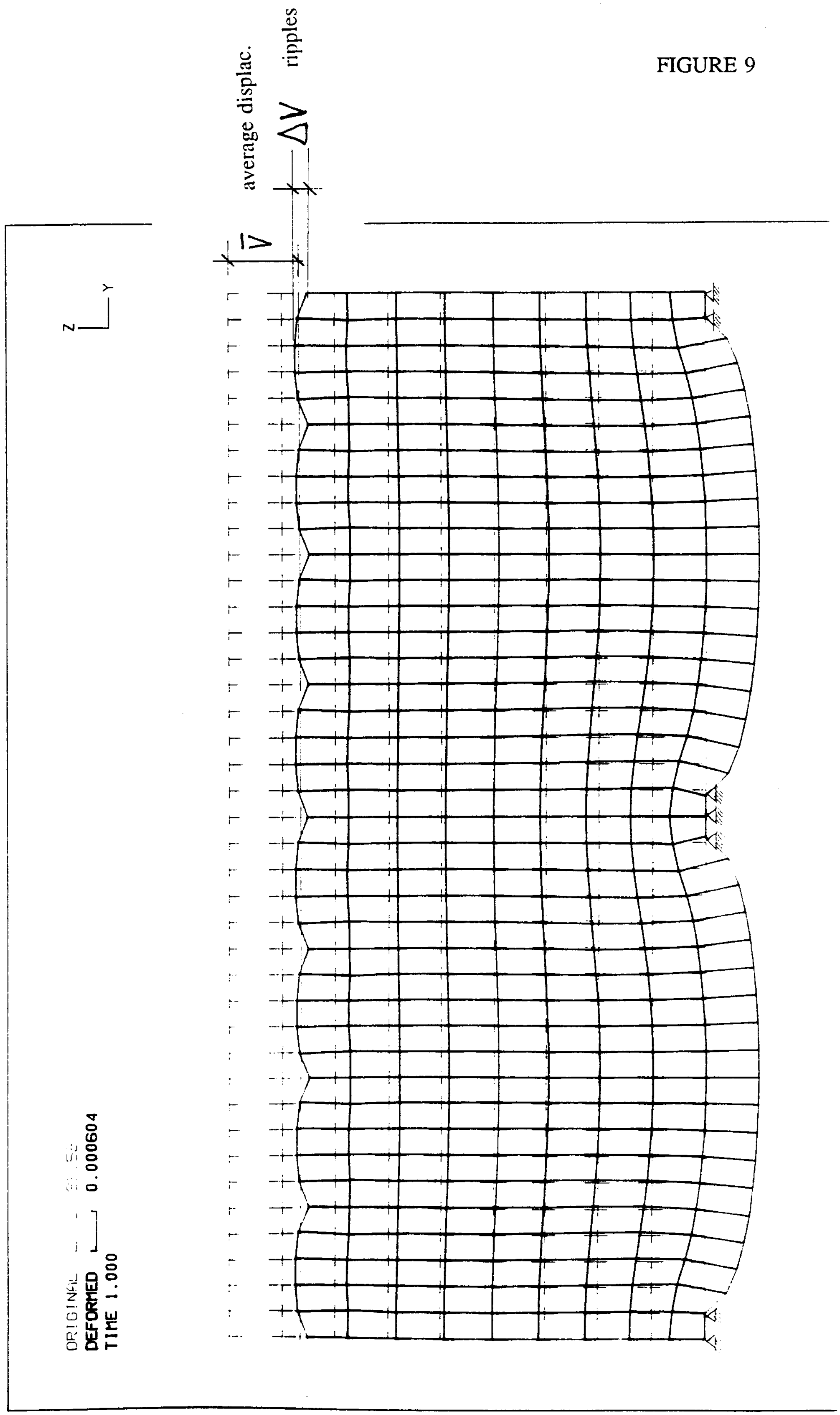

average displac.
ripples
ΔV
V̄
Z
Y
ORIGINAL
DEFORMED
TIME 1.000
0.000604

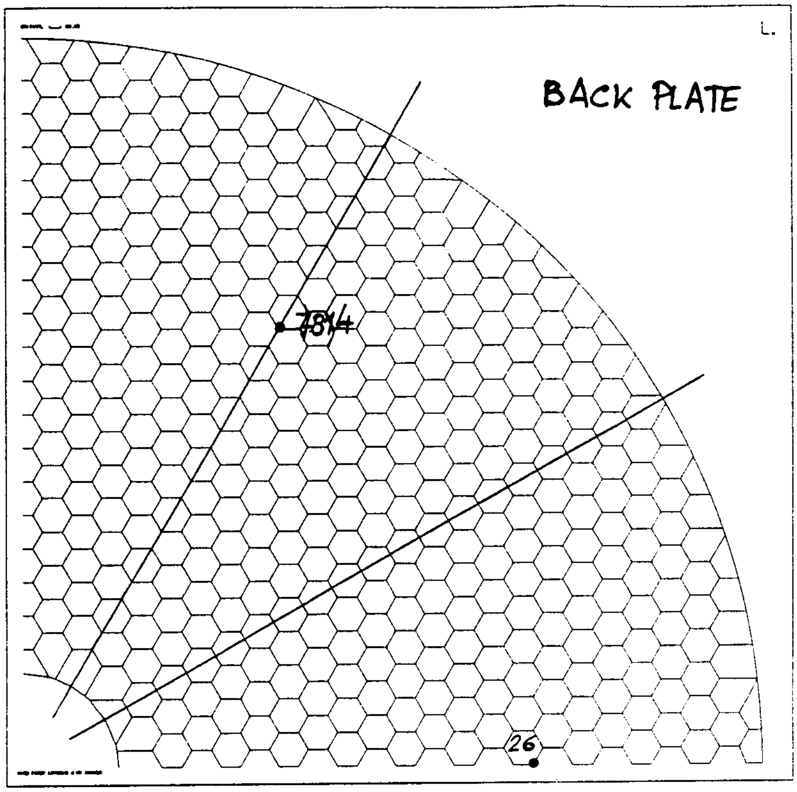

Fig. 10 - Constrains in axial direction.

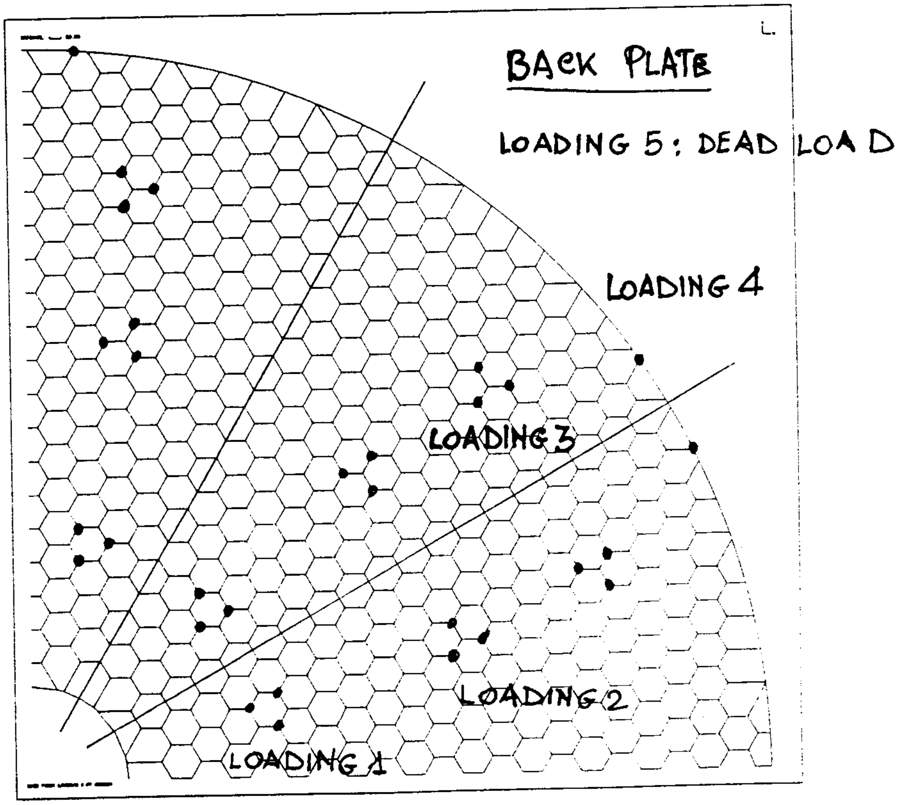

Fig. 11 - Symmetrical loads conditions.